Exploring the Potential of MnO_2 as a Material for Supercapacitors: Performance Evaluation

Arevarapu Suneel Kumar, Jayasuriya S, Venu Babu Kandru, P Srinivas Reddy*
Department for Electronics and Communication Engineering
Indian Institute of Industry Interaction Education and Research, Chennai 600066

Abstract - A new energy storage device called the supercapacitor has garnered a lot of interest because of its high energy density, quick charging and discharging times, and superior cycle stability. The selection of the electrode material has a major impact on supercapacitors' performance. Because of its remarkable qualities, which include a high theoretical specific capacitance, a wide potential range, a high degree of electrochemical activity, and its environmental friendliness, manganese dioxide (MnO_2) is regarded as a particularly promising material for electrodes. However, the material's weak conductivity and impaired volume expansion hinder its advancement and application in supercapacitors. Researchers developed porous, thin-film, or layered composite materials to increase MnO_2's specific surface area and electrical conductivity in order to solve the aforementioned issues. MnO_2 composites have been created and produced in a wide variety of forms thus far for use as supercapacitor electrodes. We present a synopsis of the latest research on MnO_2 supercapacitor electrodes in this article. We primarily focus on the techniques for fabricating these electrodes and the components that influence the MnO_2 materials' electrochemical performance. An overview of possible future directions for developing high-performance MnO_2 materials to address current problems is presented in this work.

IndexTerms - *Supercapacitors, Manganese dioxide, Carbon, and electrochemical*

I. Introduction

Energy storage devices have grown essential for supplying the intermittent energy consumption that is expanding globally. Energy storage systems need both power-dense short-term storage and energy-dense long-term storage to be sustainable. Energy storage devices are also necessary for electric vehicles in order to effectively supply power for acceleration and energy for distance travel. While capacitors can supply enormous amounts of electricity per unit volume, fuel cells and batteries can store significant amounts of energy per unit volume. The needs for energy and power are met by electrochemical capacitors and supercapacitors, which have high energy densities similar to capacitors and high power densities comparable to batteries. At the interface between the electrode and electrolyte, supercapacitors display two processes: electric double-layer capacitance (EDLC) and pseudocapacitance. According to reference, these processes add to the total specific capacitance. An electric double-layer capacitor, or EDLC, stores energy by building up charge on the electrode's surface. In contrast, the pseudo energy storage process produces a higher energy density than EDLC since it includes a quick redox reaction. A variety of carbonaceous materials, including porous charcoal, biochar, graphene, graphene oxide, reduced graphene oxide, and carbon-based nanotubes, are used in EDLCs, or electric double-layer capacitors. Owing to their substantial specific surface area, they are suitable for an extensive array of uses. Pseudocapacitor behavior is shown by metal oxides in transition states, as well as by certain sulphates and phosphates with remarkable electric, magnetic, and electrochemical properties. For redox-reaction-based pseudocapacitors, ruthenium oxide (RuO_2) and manganese oxide (MnO_2) have been explored the most. The high theoretical specific capacitance, cyclability, and power density of these oxides are well known. Since MnO_2 is the 12th most prevalent element in the crust of the Earth, it is readily available and therefore reasonably priced.
Because of its potential applications in pseudocapacitance and its technical significance, MnO_2 is a particularly interesting material. This is because it can meet energy requirements because it has several oxidative states that allow for effective charge transfer. A material's structure and morphology have a significant impact on its properties, making it possible for researchers to examine how these elements influence the material's electrochemical performance. Based on how they store charge, supercapacitors are commonly divided into two categories: pseudocapacitors and electrochemical double-layer capacitors (EDLCs). The static separation of charges in the Helmholtz layer allows energy to be stored and converted in EDLCs. Carbon-based materials make up the majority of active ingredients in double-layer electrodes. The advantage of these carbon compounds is that they maintain stability when charging and draining quickly. Nevertheless, they have relatively low capacitance and energy density—less than 10 Wh kg−1. The reason for the greater storage capacity of pseudocapacitors over EDLCs is a series of reversible redox reactions that take place within or on the surface of the electrode material. Conductive polymers and transition metal oxides are frequently utilized as pseudocapacitor electrode materials.

Supercapacitors primarily rely on the kinetics and activity of the electrode material to determine their performance. In order to improve the electrochemical properties of supercapacitors, it is vital to carefully select the right electrode materials, improve their structure, and increase their activity and kinetics. Manganese dioxide (MnO_2) and carbon compounds are commonly utilized in EDLCs and pseudocapacitors. These materials have unique advantages in terms of energy storage. The transition metal oxide MnO_2 finds widespread use in a variety of industries, including supercapacitors, aqueous batteries, oxidation catalyst materials, and others. It is selected because of its large reserves, low toxicity, and simple manufacturing process. In particular, MnO_2 is thought to be a very promising electrode material for supercapacitors. There are two main reasons behind MnO_2's remarkable performance. The single-electron redox reaction of every manganese atom is responsible for the exceptional electrochemical features of MnO_2, which include a high theoretical capacity of 1,370 F g^{-1}. Additionally, MnO_2 exhibits superior electrochemical qualities in neutral electrolyte, which minimizes the collector's chemical deterioration. MnO_2 is a plentiful, reasonably priced, and environmentally acceptable material, which makes it beneficial from an economic and environmental protection perspective. MnO_2 is an ideal choice for pseudocapacitor electrode materials due to its unique advantages. There are various crystal forms for MnO_2, including α-, β-, γ-, δ-, and λ-MnO_2.

These different crystal shapes affect the energy storage properties of MnO_2. Compared to its amorphous structure, the large surface area of δ-MnO_2, which has a layered or sheet-like structure, is more beneficial for the cation intercalation/deintercalation process. Because of its three-dimensional hinge structure, the λ-MnO_2 has more active sites and better electrochemical properties. Nevertheless, the drawbacks of MnO_2 electrode materials, such as low conductivity, insufficient ion diffusion constant, and

inadequate structural stability, limit the advancement of current MnO_2-based supercapacitors. Therefore, optimizing the active materials primarily means boosting their quick cation diffusion at high charge/discharge rates, guaranteeing structural stability, and raising their reversible capacitance. For the purpose of creating electrodes, a simple and efficient technique is to uniformly modify MnO_2 materials onto layered porous conductive functional carbon materials. Because of their interconnected pores, which promote ion diffusion, carbon materials have the potential to be extremely conductive and stable current collectors. On the other hand, MnO_2 can produce a high-performance electrode material by reducing the distance that ions must travel.

II. Review of Literature

Hybrid supercapacitors are a type of energy storage technology that offer higher power and energy density than both capacitors and batteries, according to **Afzal et al. [7].** A simple and affordable sol-gel process was used to synthesize cobalt-doped manganese oxide (Co@MnO_2), and its electrochemical properties were then assessed. 1141.42 Cg^{-1} was the specific capacity value attained, above the reference sample's value of 673.79 Cg^{-1}. At 1902 Fg^{-1}, the specific capacitance was attained. Co@MnO_2 was used to create the hybrid supercapacitor device's positive electrode, and activated carbon was used to create the negative electrode. After that, these electrodes were put together to form a two-electrode arrangement. Based on calculations, the specific capacitance of Co@MnO_2 was found to be 713.25 Fg^{-1}. The models of Randles–Ševčík and Dunn aid in the process of charge storage. It was estimated that the power density was 24 Wkg^{-1}, while the energy density was 3200 Wh kg^{-1}. After 1000 cycles of charging and discharging, this device was tested for stability, and it retained 86% of its initial capacity. Our study's conclusion provides a foundation for enhancing energy storage systems' capabilities.

A straightforward and effective hydrothermal method was presented by **Jayachandran et al. [8]** to synthesize α-MnO_2 nanorods, which might be utilized as electrode materials in high-performance supercapacitors. Using investigations utilizing High-Resolution Transmission Electron Microscopy (HR-TEM) and Powder X-ray Diffraction (XRD), the created active materials were examined for their morphological and structural properties. Through the use of Bruner-Emmert-Teller (BET) analysis and Fourier Transform-Infrared Spectroscopy (FT-IR), the functional groups and surface area properties of the α-MnO_2 nanorods were examined. Using cyclic voltammetry (CV), chromatopotentiometry (CP), and electrochemical impedance spectroscopy (EIS) studies in various aqueous electrolytes (1 M Na_2SO_4, 0.5 M KOH, and 1 M Na_2SO_4+0.5 M KOH), the electrochemical supercapacitive performance of α-MnO_2 nanorods was evaluated. The electrochemical data indicates that, in a mixed electrolyte consisting of 1 M Na_2SO_4 and 0.5 M KOH, the α-MnO_2 nanorods demonstrated a noteworthy specific capacitance of 570F/g when exposed to a current density of 1A/g.
Polyaniline-coated γ-MnO_2/carbon cloth (PANI@γ-MnO_2/CC) is a low-cost ternary hybrid material that was synthesized **by Zhu et al. [9]** using straightforward hydrothermal and in-situ electrochemical polymerization processes. Excellent qualities make the resultant material ideal for use as supercapacitor electrode material. Flexible conductive carbon fabric has the potential to function as a carbon source for γ-MnO_2 production as well as a framework for the development of PANI and γ-MnO_2. Using a range of testing techniques, the electrochemical properties and composition of the PANI@γ-MnO_2/CC composite are investigated. The three-dimensional hierarchical structure of γ-MnO_2@CC is enhanced by the application of a PANI coating layer, which also makes it easier for ions to diffuse and electrons to transfer. In a 0.5 M H_2SO_4 aqueous electrolyte, the flexible PANI@γ-MnO_2/CC composite shows a notable increase in specific capacitance, reaching 1105 mF cm^{-2} (371.4 C $g^{-1)}$ at a current density of 1 mA cm^{-2}. Furthermore, it exhibits remarkable rate performance, with capacitance retention of 72.3% when the current density is increased from 1 to 10 mA cm^{-2}, and outstanding long-term stability, retaining 86.35% capacity after 2000 cycles.

The creation of a Bi_2O_3-MnO_2 nanocomposite for use as an electrode in an electrochemical supercapacitor (ES) was reported by **Singh et al. [10].** An easy, affordable, low-temperature solid-state chemical process is used to create the nanocomposite; air annealing comes next. The process is environmentally benign. Initially, this nanocomposite's surface area, shape, phase purity, and structure were examined utilizing a variety of analytical techniques. Electrochemical analyses of the nanocomposite were then carried out. Over a wide range of potential values, the material's electrochemical performance demonstrated remarkable supercapacitive characteristics. When the material was evaluated at a current density of 1A g^{-1}, its specific capacitance reached 161 F g^{-1}. Additionally, it showed outstanding rate capability up to 10 A g^{-1}. In addition, it demonstrated remarkable cycling stability at a current density of 5 A g^{-1}, retaining 95% of its capacity even following 10,000 cycles of charge and discharge. The impressive results were observed throughout a wide potential range of 1.3 V, demonstrating the synergistic positive effects of Bi_2O_3 and MnO_2 in the Bi_2O_3-MnO_2 ES electrode. Furthermore, by building a symmetric pencil-type supercapacitor device of the Bi_2O_3-MnO_2/Bi_2O_3-MnO_2 combination, the practical reliability of the suggested electrode was verified. At a power density of 600 W kg^{-1}, this device demonstrated an energy density of 18.4 Wh kg^{-1} and continued to operate for more than three.

III. Supplies and Procedures

(1) Resources

Sigma Aldrich provided the silicon dioxide (SiO_2), potassium hydroxide (KOH), sodium sulphate (Na_2SO_4), potassium permanganate (KMnO4), and nitric acid (HNO_3). The precise materials mentioned—carbon black, polyvinylidene fluoride (PVDF), and N-methyl-2-pyrrolidone (NMP)—were acquired from Merck. When producing α-MnO_2 nanorods, premium components were used without additional purification.

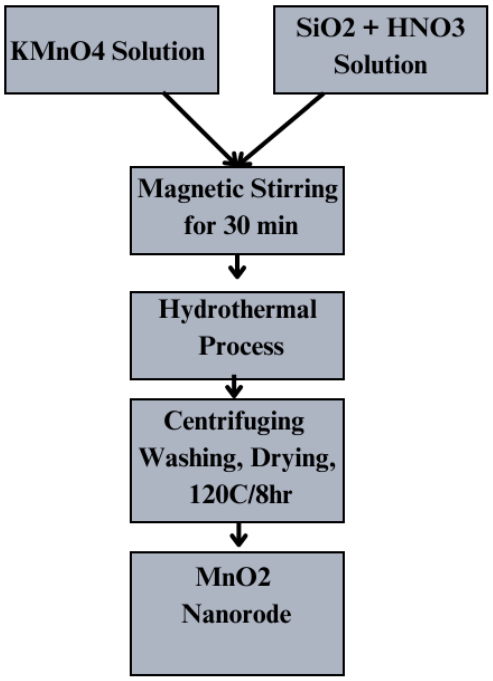

Fig 1: Hydrothermal synthesis of MnO2 nanorods

(2) MnO_2nano rod synthesis

With a few minor adjustments, the hydrothermal process previously described was used to synthesize the MnO_2 nanorods. To summarize, 60 milliliters of de-ionized water were used to dissolve 3 grams of $KMnO_4$. For thirty minutes, the solution was shaken at a steady temperature of fifty degrees Celsius. The mixture was then steadily stirred while a solution containing 0.2 grams of SiO_2 dissolved in 1 milliliter of HNO_3 was added. The solution was transferred into a 100ml Teflon-coated stainless steel autoclave once it turned purple. After the sealing procedure, the object was put inside an air oven and kept there for twelve hours at 160ºC. The solid and liquid components of the autoclave were separated by rapidly spinning it in a centrifuge once it naturally cooled to room temperature. After that, ethanol and deionized water were used to rinse the solid material to clean it. Following that, the sample was dried for eight hours at 120ºC in a hot air oven. In figure 1, the synthesis of MnO2 is shown. The thick composition, restricted porosity, and small specific surface area (<10 m^2/g) of CNFs in practical applications lead to inadequate electrochemical performance when used as electrode materials (Sun et al., 2018). As a result, they might function as a material for a MnO_2 pseudocapacitor that carries a substrate, boosting the electrode's electrochemical reaction and producing a high-performing composite electrode. As seen in Figure 1, the bubble carbon nanofibers (CNFs) were created by exploding polyacrylonitrile (PAN) at a temperature of 1,000°C. Due to the simple electron transport pathway offered by CNFs, the electrode displays a capacitance value of 428 F g^{-1} at 1 A g^{-1} after being ornamented with MnO_2 nanosheets. The composites' specific capacitance remained at 98.8% after 1,500 cycles.

(3) *Description*

The working electrodes for the electrochemical experiments were created by precisely mixing MnO_2 in an 8:1:1 ratio with activated charcoal, a binder (polyvinylidene fluoride), and a small amount of volatile organic solvent (N-methyl pyrrolidinone). After 12 hours of constant stirring, the mixture was reduced to a totally homogenous slurry. The current collector substrate was a graphite sheet to which this slurry was then put. The treated electrodes were annealed in a vacuum oven for twenty-four hours at 80 degrees Celsius. In addition, spiral Pt wires were utilized as the counter electrode and reference electrode, respectively, and Ag/AgCl wires. The experimental electrochemical measurements were conducted using the CV, GDC, and EIS methodologies. The constructed electrodes were subjected to cyclic voltammetry (CV) with an aqueous electrolyte (1 M Na_2SO_4) at various scan speeds (10–100 mVs^{-1}) and a potential range of 0.8 V. The electrode's response was investigated using electrochemical impedance spectroscopy (EIS) across a frequency range of 100 kHz to 10 mHz. The manufacturing electrode's charging and discharging properties were investigated using the GCD technique. The study employed current densities ranging from 1 to 10 A/g. Setting up a symmetrical supercapacitor apparatus: Using the same method, α-MnO_2 was directly deposited onto the graphite sheet to create the active electrode.

After the deposition process, the sample was dried in an oven for a whole day. The experiment employed active electrodes with a 1 × 1 cm^2 coated surface. These electrodes were positioned in two electrode cells with a spacer controlling the 0.25 mm spacing between them. By deducting the mass of the materials coated with the graphite sheet substrate from the mass of the uncoated materials, the loading mass (1.5 mg/cm^2) was found. Two active electrodes, a Whatman filter paper (Grade 42) separator, and an aqueous electrolyte made of a 1 M Na_2SO_4 solution were used to make the symmetric supercapacitors.

To analyze the crystal structure, phase composition, and sample purity, X-ray diffraction (XRD) was employed. The instrument used for the analysis was the BRUKER USA D8Advance, Davinci. JEOL Japan's JEM-2100 Plus High-Resolution Transmission Electron Microscope (HRTEM) was used to analyze the materials' microstructure and morphology. The Fourier Transform Infrared (FTIR) spectrum was recorded using the Perkin-Elmer Spectrum. KBr pellets were utilized in the technique, and the spectrum was acquired at a resolution of 2 cm-1 and in the 400–4000 cm–1 range. With the aid of energy dispersive spectroscopy (EDS, OXFORD 51-XMS), the material's composition was examined. Bruner-Emmert-Teller (BET) techniques were used to investigate the surface area and pore size distribution.

(4) Measurements in Electrochemistry

Three electrodes were used in the electrochemical measurements, which were carried out with the Biologic SP-300 device. Platinum wire, Hg/HgO, and α-MnO_2 coated on nickel foam were used as the counter electrode, reference electrode, and working electrode, respectively [11].

Using N-Methyl-2-pyrrolidone (NMP), a homogenous slurry was created by combining the active material (α-MnO_2), conducting additive (carbon black), and binder (PVDF) at a ratio of 85:10:5. Using the drop casting method, the slurry was applied over the nickel foam to generate a 1×1cm size electrode material for testing. The electrodes then went through a 12-hour drying procedure at 80°C. It was found that the active ingredient on the nickel foam weighed 2 mg. The frequency range used to measure the Electrochemical Impedance Spectra (EIS) was 105 Hz to 10-1 Hz. Experiments using chronopotentiometry (CP) and cyclic voltammetry (CV) were carried out across the voltage range of 0V to 0.6V. A number of aqueous electrolyte solutions, such as 1M Na_2SO_4, 0.5M KOH, and a combination electrolyte of 1M Na_2SO_4 and 0.5M KOH, were used for the aforementioned electrochemical processes. Equations (1) and (2) were utilized to determine the specific capacitance of the electrode material α-MnO_2 for the CV and CP patterns, respectively.

Equation was used to calculate the voltammetric charge integrated from the cyclic voltammogram in order to estimate the specific capacitance, or dQ/dV.

$$C_{sp}(F/g) = \frac{Q}{\Delta E \times m} \quad (1)$$

The variables are defined as follows by equation (1): Q stands for charge, measured in Coulombs (C), ΔE for potential window, measured in Volts (V), m for mass of active material, measured in grammes (g), and Csp for specific capacitance, measured in Farads per gramme (F/g).

Equation (2) can be used to approximate the specific capacity arising from the battery's charge storage behavior using the CV curves.

$$SpecificCapacity(mAh/g) = \frac{Specificcapacitance(F/g)\times\Delta E}{3.6} \quad (2)$$

In equation (2), ΔE represents the potential window, measured in volts (V).

$$C_{sp}(F/g) = \frac{I\times\Delta t}{m\times\Delta V} \quad (3)$$

The variables employed in the equation are defined as follows in equation (3): The specific capacitance is expressed as Csp, measured in Farads per gramme (F/g), the applied current is expressed as I, measured in Amperes (A), the mass of the active material is expressed as m, measured in grammes (g), the potential window is expressed as ΔV, measured in Volts (V), and the discharge duration of one cycle is expressed as Δt, measured in seconds (s).

IV. FINDINGS AND CONVERSATION

(1) X-ray Determination

X-ray diffraction was used to analyze the size and crystal structure of the generated MnO_2 phases at room temperature. Figure 2 displays the XRD spectra of every tunnelled structure created using the hydrothermal method, depending on the precursor quantity and synthesis conditions. High peaks at 2θ values of 12.7, 18.1, 28.8, 37.4, 41.9, 49.8, 56.3, 60.2, 65.1, 69.7, 72.7, and 78.5 were seen in the α-MnO2 phase (JCPDS 440141). The lattice parameters of this phase's tetragonal structure are a = 9.375 A◦ and c = 2.908 A◦. [12].

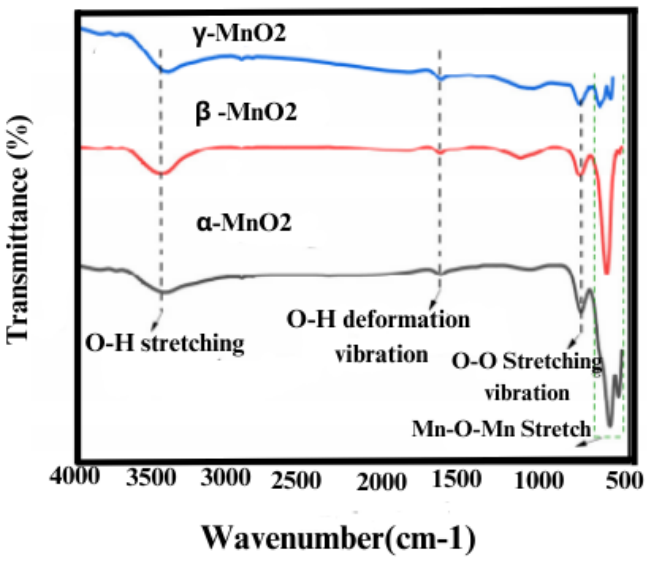

Fig 2. XRD Spectrum

It was discovered that the interplanar spacing, or d, for the (110) plane was 0.69 nm. For β-MnO_2 (rutile structure), the 2θ values that corresponded to the peaks were 28.6, 37.3, 40.9, 42.8, 46.1, 56.7, 59.3, 64.9, 67.3, and 72.4. It is possible to trace the occurrence of five distinct diffraction peaks at 2θ values of 22.2, 37.6, 42.5, 56.2, and 65.3 to γ-MnO_2, more precisely to the ramsdellite crystal structure. The γ-MnO_2-attributed peaks were semi-crystalline in form and moderately sharp. Using the Debye-Scherrer formula, the diameters of the crystallites of α-, β-, and γ-MnO_2 were found to be 19.7, 22.2, and 8 nm, respectively. The successful synthesis of many MnO_2 phases is confirmed by the XRD pattern [13].

(2) FTIR Examination

The combined FTIR spectra of all the produced MnO_2 phases are shown in Figure 3. In every polymorphous phase, the stretching vibration of O-H at 1620 cm^{-1} and the bending vibration of water at 3440 cm^{-1} were observed. The fingerprint area of the FTIR spectrum, which varied from 400 to 1600 cm^{-1}, was used to confirm the components. The measurements of peaks at 718, 524, and 476 cm−1 were used to confirm the presence of α-MnO_2. The Mn-O bond vibration was determined to be the cause of the noticeable peak observed at 524 cm^{-1}. This peak was then shifted by the Mn-O-Mn stretching vibration to 548 cm−1 for β-MnO_2 and 589 cm^{-1} for β-MnO_2, respectively. Throughout all phases, the octahedral unit (MnO_6)'s O-O stretching vibration was measured at approximately 718 cm−1. [14].

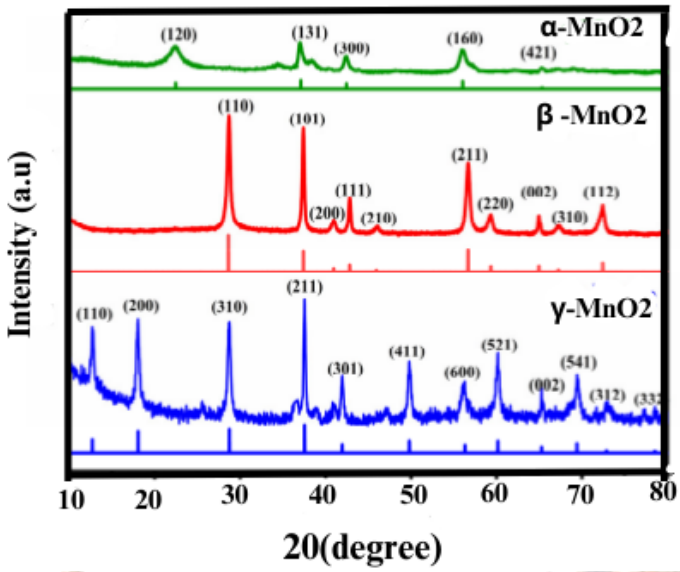

Fig 3. FTIR Spectrum.

(3) UV-Vis Analysis

The optical properties were investigated using UV-Vis absorption spectroscopy. The wavelength range covered by the study was 220–1400 nm. The findings demonstrated that, as shown in Figure 4, α-MnO_2 had a broad spectrum between 400 and 550 nm, with a peak at 416 nm. As illustrated in Figure 5, the broad spectrum of β-MnO_2 was observed between 300 and 600 nm, with a peak at 576 nm. Here was the wavelength where the highest absorption was measured. Figure 6 shows that γ-MnO_2 had a noticeable absorbance peak at 407 nm. The range of the absorbance spectrum for γ-MnO_2 was broad, extending from 300 to 600 nm. Furthermore, the direct band gaps of α-, β-, and γ- were observed to be 1.86 eV, 1.08 eV, and 1.68 eV, respectively, after the band gap was calculated using Tauc's equation. All synthesized nanostructures fall under the semiconducting material category. Because αMnO_2 has a smaller crystalline size than β-MnO_2, its band gap is larger. In addition, γ-MnO_2 has the smallest crystalline size and the lowest band gap in comparison to α-MnO_2. This may be because of its semi-crystalline structure [15].

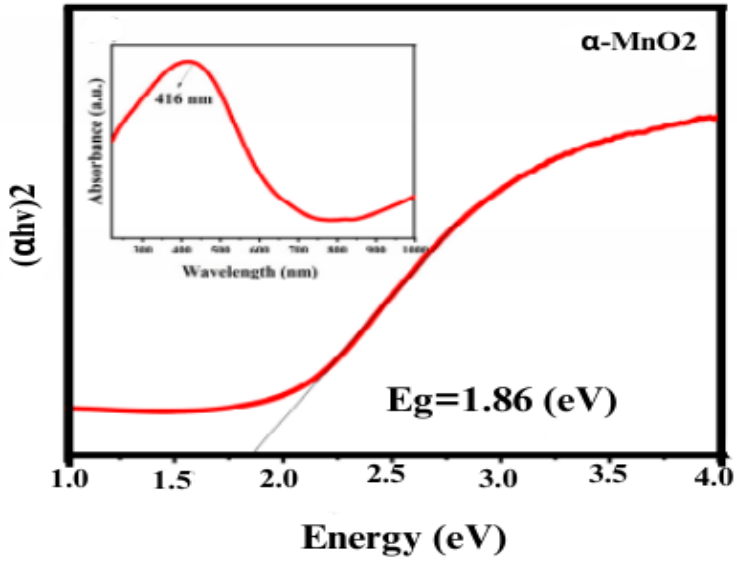

Fig 4. Tauc plot for α-MnO_2.

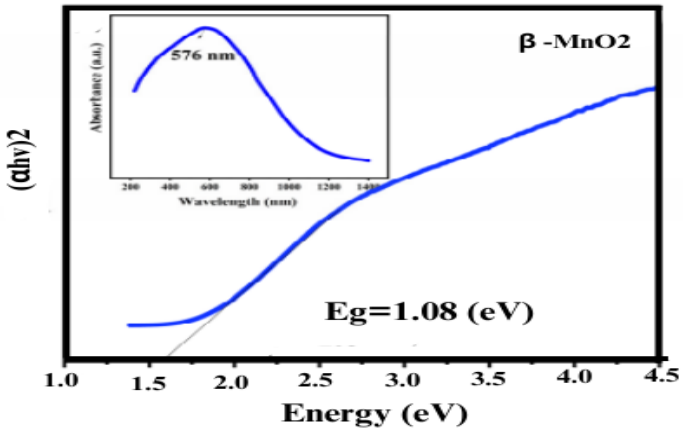

Fig 5. Tauc plot for β-MnO_2

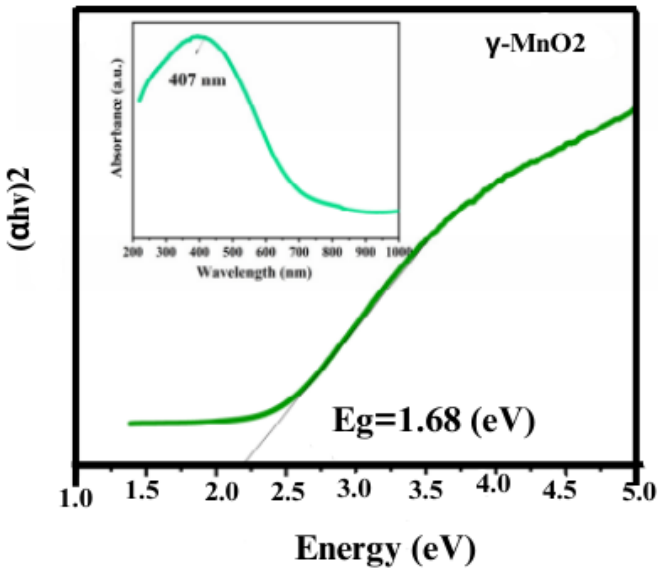

Fig 6. Tauc plot for γ-MnO_2

V. CONCLUSION

This work used a simple hydrothermal approach to synthesize MnO_2 nanorods. α-MnO_2 nanorods' electrochemical properties were investigated in three different aqueous electrolytes. The material's electrochemical behavior was shown to fluctuate in response to variations in the electrolyte, as demonstrated by the charge-discharge patterns, Nyquist plots, and cyclic voltammetry. In a mixed electrolyte liquid, the electrode material showed improved supercapacitive performance. When the electrode material was placed in a combination electrolyte solution containing 0.5 M KOH and 1 M Na_2SO_4, it demonstrated a notable specific capacitance of 570F/g at a current density of 1A/g. Over a period of 10,000 cycles, the same system demonstrated outstanding cyclic stability, with a capacity retention of 80% at a current density of 10A/g. α-MnO_2 nanorods' low resistance and excellent conductivity in a solution with 0.5 M KOH and 1 M Na_2SO_4 offer more proof that the electrolyte solution can improve the electrode material's supercapacitive behavior.

VI. References

[1] Cao, J., Li, X., Wang, Y., Walsh, F.C., Ouyang, J.H., Jia, D. and Zhou, Y., 2015. Materials and fabrication of electrode scaffolds for deposition of MnO2 and their true performance in supercapacitors. Journal of Power Sources, 293, pp.657-674.

[2] Majumdar, D., 2021. Review on current progress of MnO2-based ternary nanocomposites for supercapacitor applications. ChemElectroChem, 8(2), pp.291-336.

[3] Zhao, Y., Meng, Y. and Jiang, P., 2014. Carbon@ MnO2 core–shell nanospheres for flexible high-performance supercapacitor electrode materials. Journal of Power Sources, 259, pp.219-226.

[4] Sadak, O., Wang, W., Guan, J., Sundramoorthy, A.K. and Gunasekaran, S., 2019. MnO2 nanoflowers deposited on graphene paper as electrode materials for supercapacitors. ACS Applied Nano Materials, 2(7), pp.4386-4394.

[5] Deshmukh, P.R., Sohn, Y. and Shin, W.G., 2018. Electrochemical performance of facile developed aqueous asymmetric (Fe, Cr) 2O3//MnO2 supercapacitor. ElectrochimicaActa, 285, pp.381-392.

[6] Xu, L., Jia, M., Li, Y., Jin, X. and Zhang, F., 2017. High-performance MnO2-deposited graphene/activated carbon film electrodes for flexible solid-state supercapacitor. Scientific reports, 7(1), p.12857.

[7] Afzal, A.M., Muzaffar, N., Iqbal, M.W., Dastgeer, G., Manzoor, A., Razaq, M., Wabaidur, S.M., Al-Ammar, E.A. and Eldin, S.M., 2024. Exploring the charge storage mechanism in high-performance Co@ MnO2-based hybrid supercapacitors using Randles–Ševčík and Dunn's models. Journal of Applied Electrochemistry, 54(1), pp.65-76.

[8] Jayachandran, M., Rose, A., Maiyalagan, T., Poongodi, N. and Vijayakumar, T., 2021. Effect of various aqueous electrolytes on the electrochemical performance of α-MnO2 nanorods as electrode materials for supercapacitor application. Electrochimicaacta, 366, p.137412.

[9] Zhu, Y., Xu, H., Chen, P., Bao, Y., Jiang, X. and Chen, Y., 2022. Electrochemical performance of polyaniline-coated γ-MnO2 on carbon cloth as flexible electrode for supercapacitor. ElectrochimicaActa, 413, p.140146.

[10] Singh, S., Sahoo, R.K., Shinde, N.M., Yun, J.M., Mane, R.S. and Kim, K.H., 2019. Synthesis of Bi2O3-MnO2 nanocomposite electrode for wide-potential window high performance supercapacitor. Energies, 12(17), p.3320.

[11] Su, X., Yu, L., Cheng, G., Zhang, H., Sun, M. and Zhang, X., 2015. High-performance α-MnO2 nanowire electrode for supercapacitors. Applied energy, 153, pp.94-100.

[12] Wang, J.G., Kang, F. and Wei, B., 2015. Engineering of MnO2-based nanocomposites for high-performance supercapacitors. Progress in Materials Science, 74, pp.51-124.

[13] Bhat, T.S., Jadhav, S.A., Beknalkar, S.A., Patil, S.S. and Patil, P.S., 2022. MnO2 core-shell type materials for high-performance supercapacitors: a short review. Inorganic Chemistry Communications, 141, p.109493.

[14] Liu, Juyin, JialiBao, Xin Zhang, YanfangGao, Yao Zhang, Ling Liu, and Zhenzhu Cao. "MnO 2-based materials for supercapacitor electrodes: challenges, strategies and prospects." RSC advances 12, no. 55 (2022): 35556-35578.

[15] Zhang, Q.Z., Zhang, D., Miao, Z.C., Zhang, X.L. and Chou, S.L., 2018. Research progress in MnO2–carbon based supercapacitor electrode materials. Small, 14(24), p.1702883.